Joint Estimation of DOA and Carrier Frequency Based on Coprime Arrays

Kai-Chieh Hsu and Jean-Fu Kiang*

Department of Electrical Engineering

Nation Taiwan University

Outline

- Introduction
- Proposed methods
- Simulations and discussions
- Conclusion

DOA estimation algorithms

- Conventional algorithms
  - Multiple Signal Classification (MUSIC) [1]
  - Estimation of Signal Parameters via Rotational Invariance Techniques (ESPRIT) [2]
- Increase degrees of freedom (DOFs)
  - Khatri-Rao subspace (KR) [3]
  - Coprime array (CPA) [4], [5]

[1] R. Schmidt, "Multiple emitter location and signal parameter estimation," *IEEE Trans. Antennas Propagat.*, vol. 34, no.3, pp. 276-280, 1986.
[2] R. Roy and T. Kailath, "ESPRIT-estimation of signal parameters via rotational invariance techniques," *IEEE Trans. Acous. Speech Signal Process.*, vol. 37, no.7, pp. 984-995, 1989.
[3] W. K. Mao, T. H. Hsieh and C. Y. Chi, "DOA estimation of quasi-stationary signals with less sensors than sources and unknown spatial noise covariance: A Khatri-Rao subspace approach," *IEEE Trans. Signal Process.*, vol. 58, no. 4, pp. 2168-2180, 2010.
[4] P. Pal and P. P. Vaidyanathan, "Coprime sampling and the MUSIC algorithm," *Proc. IEEE DSP/SPE* Workshop, pp. 289-294, 2011.
[5] S. Qin, Y. D. Zhang and M. G. Amin, "Generalized coprime array configurations for direction-of-arrival estimation," *IEEE Trans. Signal Process.*, vol. 63, no. 6, pp. 1377-1390, 2015.

Co-prime Array (CPA)

- Array configuration
  - Subarray 1 is composed of $2N_1$ sensors at spacing $N_2 d$.
  - Subarray 2 is composed of N_2 sensors at spacing $N_1 d$.
  - Total $2N_1 + N_2 - 1$ sensors in the CPA.

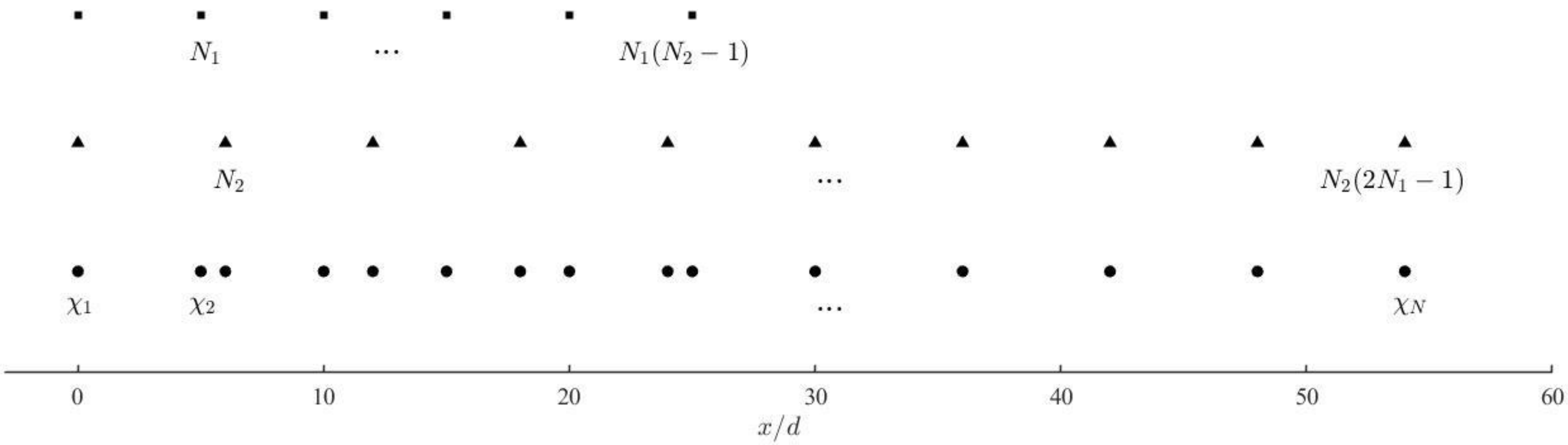

Fig. 1. Configuration of CPA

DOF of Co-prime Array

- DOFs are increased to
  - $3N_1N_2 + N_1 - N_2$ unique virtual sensors
  - $N_1N_2 + N_1 - 1$ consecutive virtual sensors

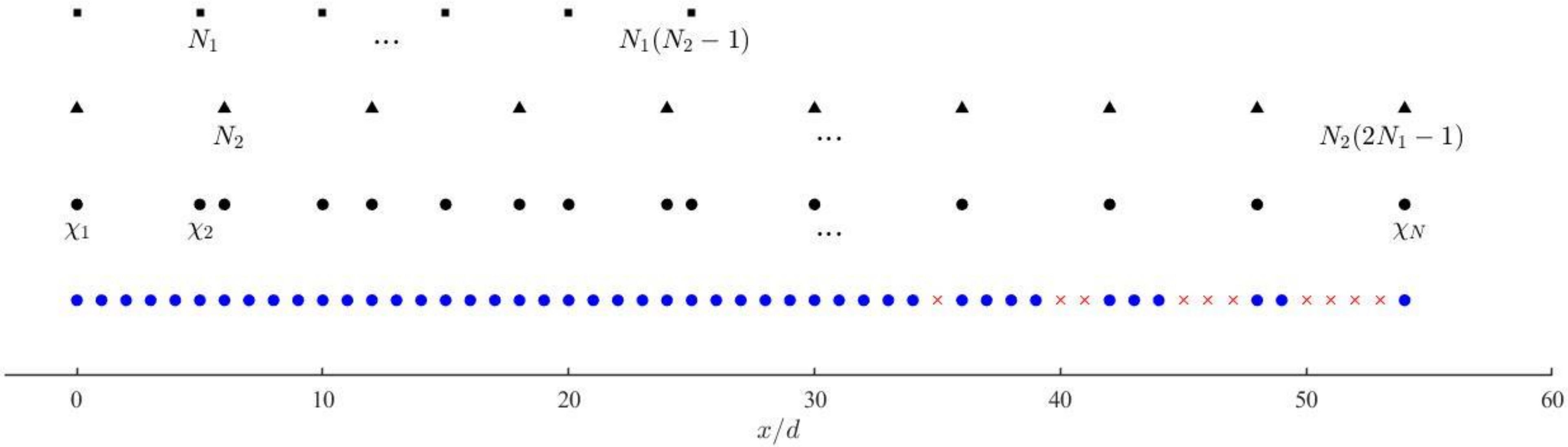

Joint ESPRIT (1/2) [6]

- Above mentioned DOA estimation algorithms require known CF.
- A Joint ESPRIT (JE) was proposed to estimate both DOA and CF.
- Consider there are two L snapshots of the measurements $\bar{x}$ and $\bar{z}$ along the x and z axis, which are divided into two sub-vectors, respectively.

$$\bar{x}_1 = \bar{x}[1:L-1],\ \bar{x}_2 = \bar{x}[2:L]$$
$$\bar{z}_1 = \bar{z}[1:L-1],\ \bar{z}_2 = \bar{z}[2:L]$$

- Estimate four covariance matrices

$$\bar{\bar{\mathrm{R}}}_1 = \sum_{\ell=1}^{L-1} \bar{x}_1[\ell]\, \bar{z}_1^{\dagger}[\ell],\ \bar{\bar{\mathrm{R}}}_2 = \sum_{\ell=1}^{L-1} \bar{x}_2[\ell]\, \bar{z}_1^{\dagger}[\ell]$$
$$\bar{\bar{\mathrm{R}}}_3 = \sum_{\ell=1}^{L-1} \bar{x}_2[\ell]\, \bar{z}_1^{\dagger}[\ell],\ \bar{\bar{\mathrm{R}}}_4 = \sum_{\ell=1}^{L-1} \bar{x}_2[\ell]\, \bar{z}_2^{\dagger}[\ell]$$

[6] S. Stein Ioushua, O. Yair, D. Cohen, and Y. C. Eldar, “CaSCADE: Compressed Carrier and DOA Estimation,” in IEEE Trans. Signal Process., vol. 65, no. 10, pp. 2645-2658, 2017.

Joint ESPRIT (2/2) [6]

- Apply SVD on $\bar{\bar{R}} = \left[\bar{\bar{\mathrm{R}}}_1^T \quad \bar{\bar{\mathrm{R}}}_2^T \quad \bar{\bar{\mathrm{R}}}_3^T \quad \bar{\bar{\mathrm{R}}}_4^T \right]^T = \bar{\bar{U}}\, \bar{\bar{\Sigma}}\, \bar{\bar{V}}^\dagger$ and construct

$$\bar{\bar{U}}_{s1} = \bar{\bar{U}}[1{:}N-1, 1{:}M], \bar{\bar{U}}_{s2} = \bar{\bar{U}}[N{:}2N-2, 1{:}M]$$

$$\bar{\bar{U}}_{s3} = \bar{\bar{U}}[2N-1{:}3N-3, 1{:}M], \bar{\bar{U}}_{s4} = \bar{\bar{U}}[3N-2{:}4N-4, 1{:}M]$$

- Compute

$$\bar{\bar{U}}_{12} = \bar{\bar{U}}_{s1}^{-1}\, \bar{\bar{U}}_{s2}, \bar{\bar{U}}_{13} = \bar{\bar{U}}_{s1}^{-1}\, \bar{\bar{U}}_{s3}, \bar{\bar{U}}_{14} = \bar{\bar{U}}_{s1}^{-1}\, \bar{\bar{U}}_{s4}$$

and apply EVD on $\bar{\bar{\Omega}} = \frac{(\bar{\bar{U}}_{12} + \bar{\bar{U}}_{13} + \bar{\bar{U}}_{14})}{3} = \bar{\bar{T}}^{-1}\, \bar{\bar{\Lambda}}\, \bar{\bar{T}}$.

- Compute

$$\bar{\bar{\Psi}}_x = \bar{\bar{T}}\, \bar{\bar{U}}_{12}\, \bar{\bar{T}}^{-1}, \bar{\bar{\Psi}}_z = \left(\bar{\bar{T}}\, \bar{\bar{U}}_{13}\, \bar{\bar{T}}^{-1} \right)^\dagger$$

- Estimate DOA and CF as

$$\theta_m = \tan^{-1} \frac{\angle \bar{\bar{\Psi}}_{z,m}}{\angle \bar{\bar{\Psi}}_{x,m}}, f_m = \frac{c}{2\pi d} \sqrt{\left(\angle \bar{\bar{\Psi}}_{x,m}\right)^2 + \left(\angle \bar{\bar{\Psi}}_{z,m}\right)^2}$$

where $\bar{\bar{\Psi}}_{x,m}$ and $\bar{\bar{\Psi}}_{z,m}$ is the mth diagonal entry of $\bar{\bar{\Psi}}_x$ and $\bar{\bar{\Psi}}_z$, respectively.

Sensor Arrays

- Consider two orthogonal CPAs(5,6) along x and z axes, respectively.

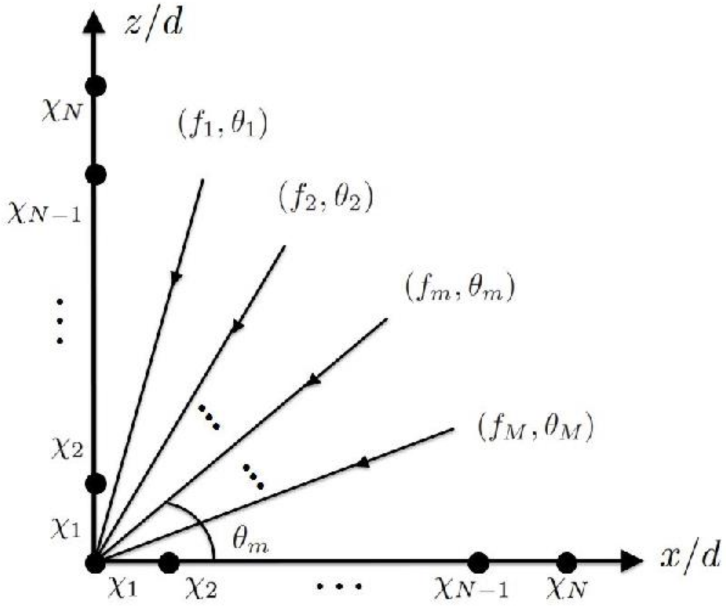

Fig. 2. Two orthogonal CPAs along x and z axes

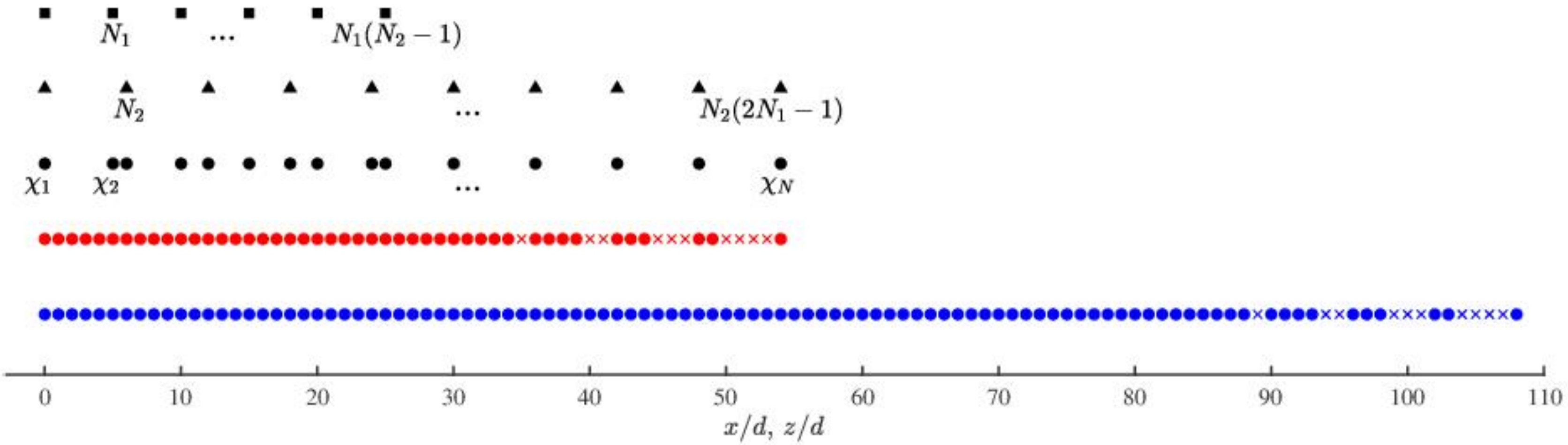

Fig. 3. Configuration, second-order and fourth-order virtual arrays of CPA

Signal Model

- Consider source signals are mixed of CF-known and CF-unknown.
- Received data: $\bar{\bar{X}}, \bar{\bar{Z}} \in \mathbb{C}^{N \times LQ}$, where N is the number of sensors, Q is the number of observed time frames and L is the length of each time frame.
- Each column of $\bar{\bar{X}}, \bar{\bar{Z}}$ is composed of received signals from CPA in x and z axes, respectively.

$$\bar{x}[\ell] = \bar{\bar{X}}[:,\ell] = \bar{\bar{A}}_x \cdot \bar{s}[\ell] + \bar{n}_x[\ell],$$
$$\bar{z}[\ell] = \bar{\bar{Z}}[:,\ell] = \bar{\bar{A}}_z \cdot \bar{s}[\ell] + \bar{n}_z[\ell].$$

Second-order manifold signals

- Construct covariance matrix as

$$\bar{\bar{R}}_x^q = \Sigma_{\ell=1}^{\mathrm{L}} \bar{x}^q[\ell]\bar{x}^{q\dagger}[\ell],\ \bar{\bar{R}}_z^q = \Sigma_{\ell=1}^{\mathrm{L}} \bar{z}^q[\ell]\bar{z}^{q\dagger}[\ell]$$

where $\bar{x}^q[\ell] = \bar{x}[(q-1)L+\ell]$ and $\bar{z}^q[\ell] = \bar{z}[(q-1)L+\ell]$.

- Second-order manifold signals:
  - Vectorize:

$$\bar{y}_x'[q] = Vec\{\bar{\bar{R}}_x^q\},\ \bar{y}_z'[q] = Vec\{\bar{\bar{R}}_z^q\}$$

with entries corresponding to the same lags are averaged.

  - Subtract Bias:

$$\bar{y}_x[q] = \bar{y}_x'[q] - \Sigma_{q=1}^{Q}\bar{y}_x'[q],\ \bar{y}_z[q] = \bar{y}_z'[q] - \Sigma_{q=1}^{Q}\bar{y}_z'[q]$$

Fourth-order manifold signals

- Construct fourth-order manifold signals as

$$\bar{\bar{R}}_{xx} = \frac{1}{Q}\Sigma_{q=1}^{Q}\bar{y}_x[q]\,\bar{y}_x^{\dagger}[q],\ \bar{y}_{xx} = Vec\{\bar{\bar{R}}_{xx}\}$$

$$\bar{\bar{R}}_{zz} = \frac{1}{Q}\Sigma_{q=1}^{Q}\bar{y}_z[q]\,\bar{y}_z^{\dagger}[q],\ \bar{y}_{zz} = Vec\{\bar{\bar{R}}_{zz}\}$$

- MUSIC or ESPRIT cannot be directly applied to.
- Spatial-Smoothing MUSIC (SSM) is applied.

Dimension-reduced method

- Before applying SSM to solve for the DOA, a dimension-reduced method is used to
- The number of overlapped lags in the second-order covariance matrix is small, but that of the fourth-order covariance matrix is large.
- The overlapped lags of each entry in $\bar{\bar{R}}_{xx}$ and $\bar{\bar{R}}_{zz}$ is recorded in a dictionary (Φ).
- By taking the average of entries with the same lag and removing them, dimension-reduced fourth-order manifold signals are formed as $\bar{y}_{xx}^{\Phi}$ and $\bar{y}_{zz}^{\Phi}$.

First-Step: DOA of CF-known Sources Spatial-Smoothing MUSIC [4]

- SSM requires the received signal vector be derived from consecutive lags, which is extracted from $\bar{y}_{xx}^{\Phi}$ and $\bar{y}_{zz}^{\Phi}$ and SSM matrices are constructed as

$$\bar{\bar{R}}'_{xx} = \begin{bmatrix} \bar{y}_{xx}^{\Phi}[1] & \bar{y}_{xx}^{\Phi}[2] & & \bar{y}_{xx}^{\Phi}[N_f+1] \\ \bar{y}_{xx}^{\Phi}[2] & \bar{y}_{xx}^{\Phi}[3] & \cdots & \bar{y}_{xx}^{\Phi}[N_f+2] \\ \vdots & \vdots & & \vdots \\ \bar{y}_{xx}^{\Phi}[N_f+1] & \bar{y}_{xx}^{\Phi}[N_f+2] & & \bar{y}_{xx}^{\Phi}[2N_f+1] \end{bmatrix}$$

$$\bar{\bar{R}}'_{zz} = \begin{bmatrix} \bar{y}_{zz}^{\Phi}[1] & \bar{y}_{zz}^{\Phi}[2] & & \bar{y}_{zz}^{\Phi}[N_f+1] \\ \bar{y}_{zz}^{\Phi}[2] & \bar{y}_{zz}^{\Phi}[3] & \cdots & \bar{y}_{zz}^{\Phi}[N_f+2] \\ \vdots & \vdots & & \vdots \\ \bar{y}_{zz}^{\Phi}[N_f+1] & \bar{y}_{zz}^{\Phi}[N_f+2] & & \bar{y}_{zz}^{\Phi}[2N_f+1] \end{bmatrix}$$

Where $N_f = 3N_1N_2 + N_1 - N_2 - 1$ is the number of positive lags.

- The MUSIC is then applied to the SSM matrix to estimate DOA of CF-known sources with a simple pairing method.

Second-Step: Joint DOA and CF Estimation Projected Joint-ESPRIT (PJE)

- With estimated DOA of CF-known sources, we can remove them by orthogonal complement projectors constructed as

$$\bar{\bar{\Pi}}_x = \bar{\bar{I}} - \bar{\bar{B}}_x \cdot (\bar{\bar{B}}_x^{\dagger} \cdot \bar{\bar{B}}_x)^{-1} \cdot \bar{\bar{B}}_x^{\dagger},$$

$$\bar{\bar{\Pi}}_z = \bar{\bar{I}} - \bar{\bar{B}}_z \cdot (\bar{\bar{B}}_z^{\dagger} \cdot \bar{\bar{B}}_z)^{-1} \cdot \bar{\bar{B}}_z^{\dagger}.$$

- Projected second-order manifold signals

$$\bar{y}_x''[q] = \bar{\bar{\Pi}}_x \cdot \bar{y}_x[q],$$

$$\bar{y}_z''[q] = \bar{\bar{\Pi}}_z \cdot \bar{y}_z[q].$$

- Then, joint-ESPRIT can be directly applied.

Simulation Setting

- The length of each time frame is randomly pick from $Unif[300,700]$.
- Half of the DOAs are at uniform spacing between $[-20^{\circ}, -70^{\circ}]$ and $[20^{\circ}, 70^{\circ}]$, respectively.
- In each scenario, 200 Monte Carlo realizations are simulated.

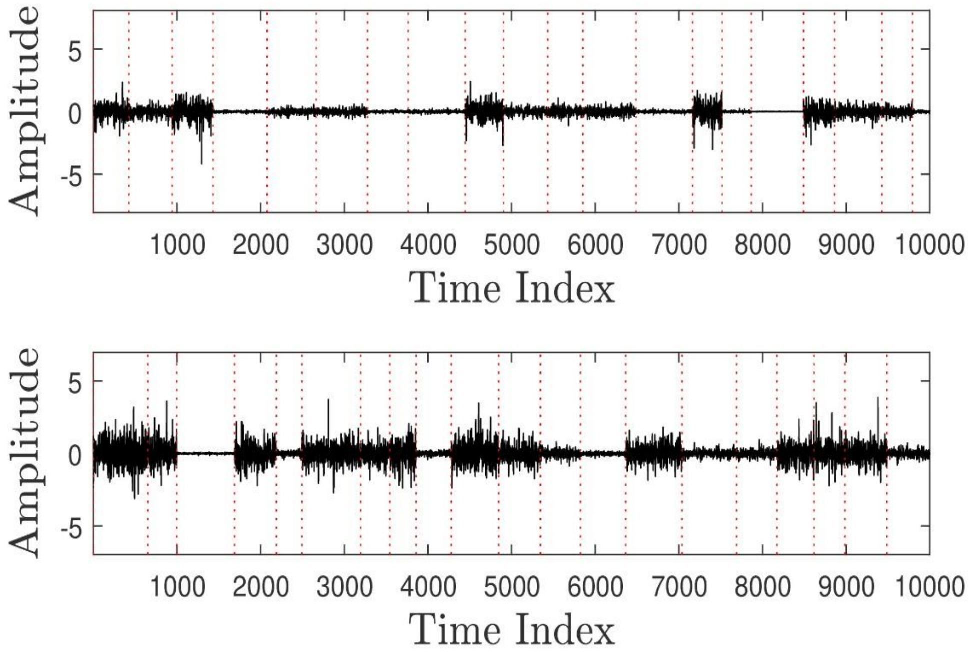

Fig. 4. Source Signals

RMSE versus M_u

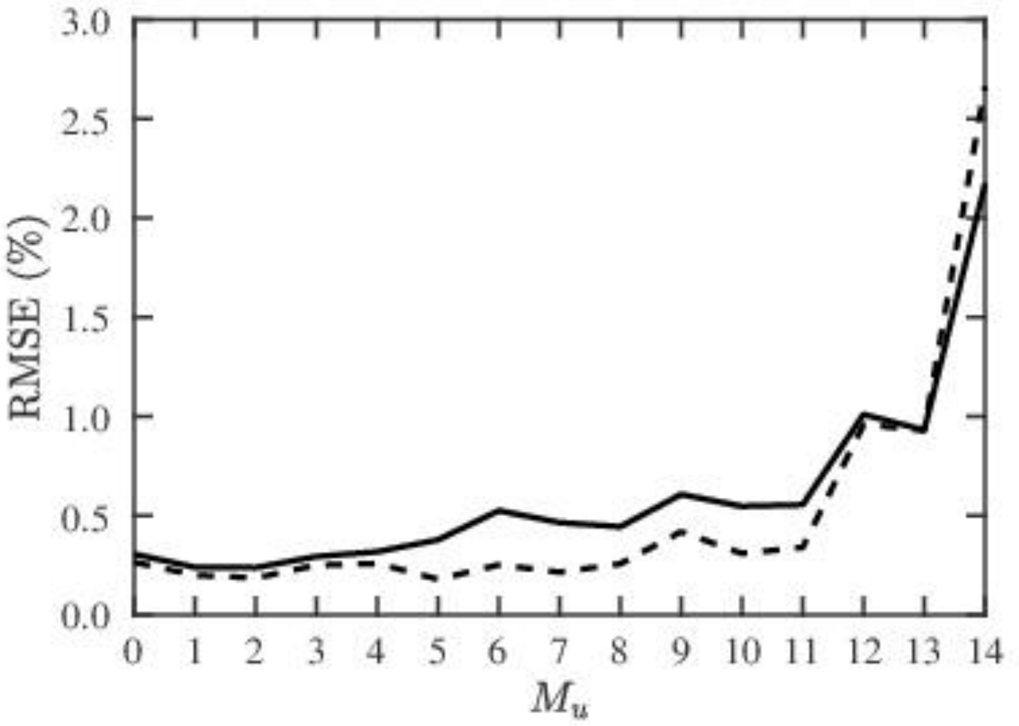

Fig. 5: RMSE of DOA and CF estimation with proposed PJE algorithm, under different number of signals with unknown CF, SNR = 10 dB, Q = 300, M = 30. ———:RMSE of DOA, – – –: RMSE of CF.

- Proposed two-stage algorithm works reasonably well if $M_u \leq 11$
- RMSEs increase dramatically when $M_u \geq 13$, indicating that the maximum number of CF-unknown sources is about 13 in this case.

SSM Spectrum

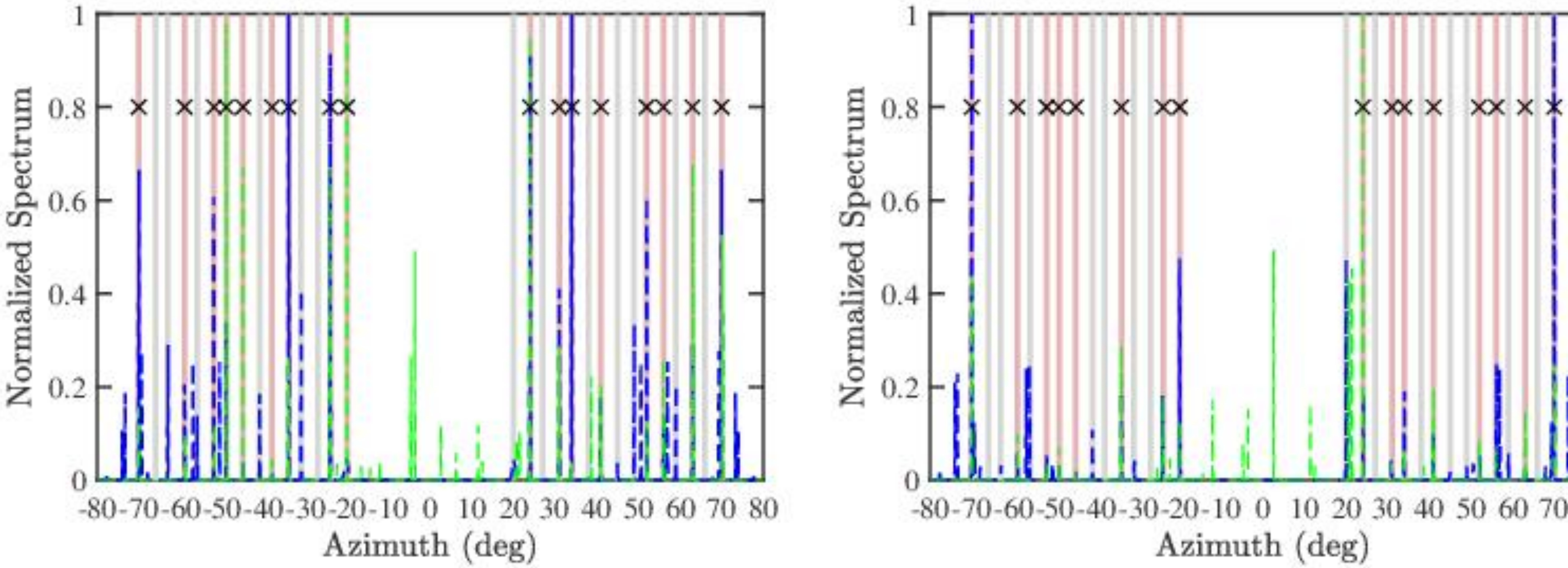

Fig. 6: Normalized SS-MUSIC spectrum (left) M_u = 13 and (right) M_u = 14, SNR = 10 dB, Q = 300,M = 30. Gray lines: actual DOAs of CF-known, Red lines: actual DOAs of CF-unknown, Blue dashed lines: Estimated DOAs based on x-axis, Green dashed lines: Estimated DOAs based on z-axis, ×: pairing DOAs.

- All the CF-known sources are correctly estimated in both cases →The problems arise from CF-unknown sources estimation.

Estimation of PJE

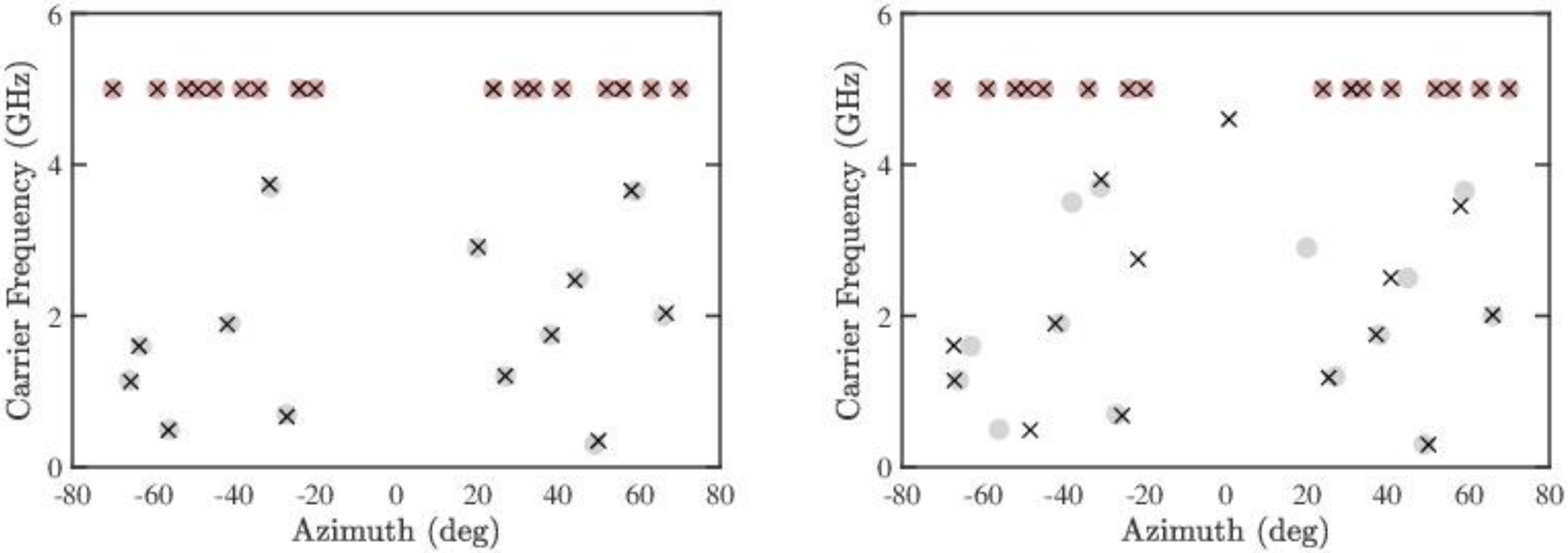

Fig. 7: Joint estimation of DOA and CF with proposed PJE algorithm, (left) M_u = 13 and (right) M_u = 14, SNR = 10 dB, Q = 300, M = 30.•: CF-known sources, •:CF-unknown sources, ×: estimated sources.

- This observation confirms that the maximum number of detectable CF-unknown sources is 13 in this case.

Estimation of PJE vs JE

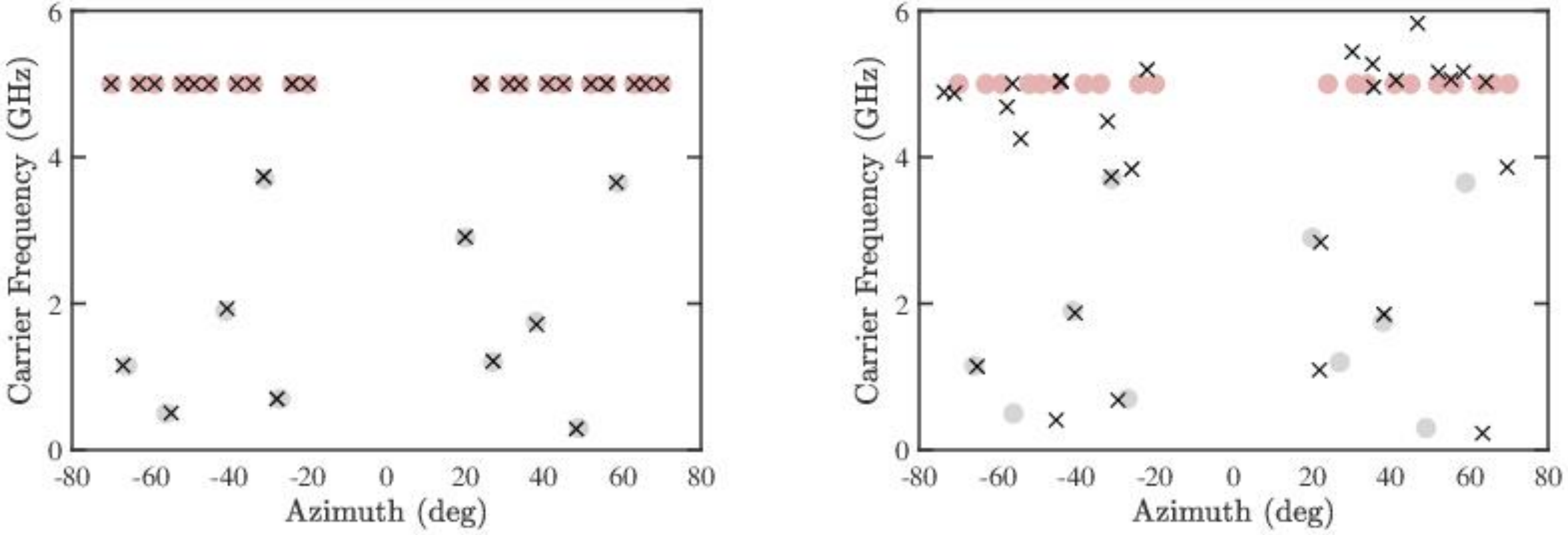

Fig. 8: Joint estimation of DOA and CF, SNR = 10 dB, Q = 300, M = 30, M_u = 10. (left) Proposed PJE algorithm (right) conventional JE algorithm. •: CF-known sources, •:CF-unknown sources, ×: estimated sources.

- Proposed PJE algorithm can detect all the sources accurately.
- The error of CF-known sources is higher than that of CF-unknown sources in the JE. One possible reason is that joint diagonalization in the conventional JE algorithm probably decreases phase resolution, which is more required in CF-known sources since the delay difference is quite small.

RMSE versus SNR

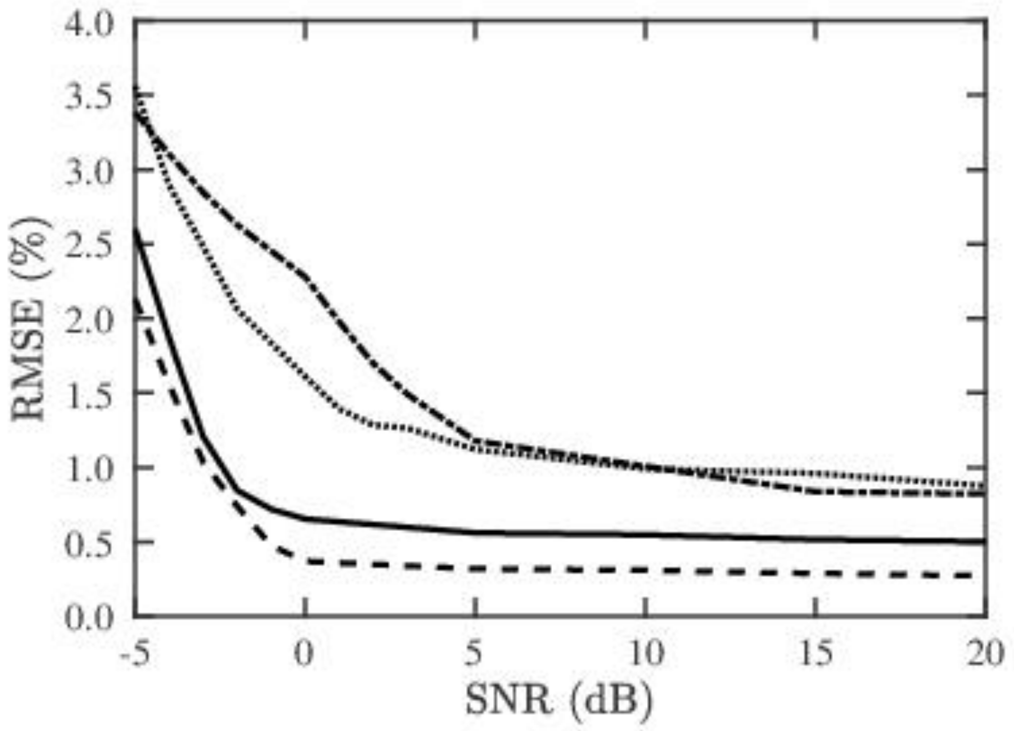

Fig. 9: RMSE of DOA and CF estimation versus SNR, with proposed PJE algorithm, Mu = 10, Q = 300, M =30.
———: RMSE of DOA with Mu = 10,
– – –: RMSE of CF with Mu = 10,
–·–: RMSE of DOA with Mu = 13,
· · · : RMSE of CF with Mu = 13.

- well below 1 % at SNR > 0 dB if Mu = 10
- below 1 % at SNR > 5 dB if Mu = 13

Conclusion

- A two-step method is proposed to estimate the DOA of multiple targets from the received signals originated from a mix of CF-known and CF-unknown sources.
- In the first step, SSM method with a simple pairing is applied to estimate DOAs of CF-known sources.
- In the second step, orthogonal complement projectors are used to remove CF-known sources and then joint-ESPRIT is applied to jointly estimate DOA and CF of CF-unknown sources.
- Simulation results demonstrate our proposed method can detect all 30 sources with 13 M_u and outperforms conventional JE.